

Out-of-equilibrium critical dynamics of the three-dimensional \mathbb{Z}_2 gauge model along critical relaxational flows

Claudio Bonati,¹ Haralambos Panagopoulos,² and Ettore Vicari³

¹*Dipartimento di Fisica dell'Università di Pisa and INFN, Largo Pontecorvo 3, I-56127 Pisa, Italy*

²*Department of Physics, University of Cyprus, P.O. Box 20537, 1678 Nicosia, Cyprus*

³*Dipartimento di Fisica dell'Università di Pisa, Largo Pontecorvo 3, I-56127 Pisa, Italy*

(Dated: January 20, 2025)

We address the out-of-equilibrium critical dynamics of the three-dimensional lattice \mathbb{Z}_2 gauge model, and in particular the critical relaxational flows arising from instantaneous quenches to the critical point, driven by purely relaxational (single-spin-flip Metropolis) upgradings of the link \mathbb{Z}_2 gauge variables. We monitor the critical relaxational dynamics by computing the energy density, which is the simplest local gauge-invariant quantity that can be measured in a lattice gauge theory. The critical relaxational flow of the three-dimensional lattice \mathbb{Z}_2 gauge model is analyzed within an out-of-equilibrium finite-size scaling framework, which allows us to compute the dynamic critical exponent z associated with the purely relaxational dynamics of the three-dimensional \mathbb{Z}_2 gauge universality class. We obtain $z = 2.610(15)$, which significantly improves earlier results obtained by other methods, in particular those obtained by analyzing the equilibrium critical dynamics.

I. INTRODUCTION

Gauge symmetries are crucial features of effective theories that describe collective phenomena developing topological transitions, driven by extended charged excitations with nonlocal order parameters, or by a nontrivial interplay between long-range scalar fluctuations and nonlocal topological gauge modes. Examples of such transitions are observed in lattice gauge theories with discrete \mathbb{Z}_N and continuous $U(1)$ gauge symmetries, see, e.g., Refs. [1–4] for recent reviews. While the static critical properties in the presence of gauge symmetries have been much investigated, see, e.g., Refs. [5–49], achieving a satisfactory understanding of the various critical scenarios that can be realized [2], much less is known about their critical dynamics in both equilibrium and out-of-equilibrium conditions. We believe that extending our knowledge of the critical scenarios to dynamic, equilibrium and out-of-equilibrium, situations may lead to a deeper understanding of the mechanisms underlying topological transitions in the presence of gauge symmetries. We recall that a fair understanding of the critical dynamics has been already achieved in the case of classical and quantum many-body systems without gauge symmetries, see, e.g., Refs. [50–55].

The three-dimensional (3D) \mathbb{Z}_2 gauge model [5] is a paradigmatic lattice system undergoing a finite-temperature topological transition without any local order parameter [2, 4, 5], separating the high-temperature deconfined phase from the low-temperature confined phase. By duality [5, 10], this model can be related to the standard 3D Ising model (in the absence of external magnetic fields breaking the \mathbb{Z}_2 symmetry), implying that their static critical behaviors share analogous asymptotic behaviors for the diverging length scale ξ of their critical correlations, $\xi \sim |T - T_c|^{-\nu}$ with $\nu \approx 0.630$ [56].

The equilibrium and out-of-equilibrium dynamics at continuous transitions is generally affected by critical

slowing down. The time scale of the critical modes diverges as $\tau \sim \xi^z$, where z is an independent dynamic exponent, whose value also depends on the type of dynamics [51, 53]. The simplest example is provided by the purely relaxational dynamics associated with a stochastic Langevin equation where only dissipative couplings are present, with no conservation laws, usually called dynamic model A [50, 51]. In lattice models the purely relaxational dynamics can be realized by standard Metropolis upgradings of the lattice variables [57].

Despite the fact that 3D \mathbb{Z}_2 gauge and Ising spin models share the same static critical behavior, they exhibit different critical dynamics under local relaxational upgradings. Indeed the time scale of their critical modes develop different power laws, as shown by some numerical analyses of the purely relaxational dynamics, under equilibrium and out-of-equilibrium conditions [58–60]. The most recent results for the dynamic exponent z of the purely relaxational dynamics of the 3D \mathbb{Z}_2 gauge model are $z = 2.55(6)$, obtained by analyzing the critical relaxational dynamics of model in equilibrium conditions [60], and $z = 2.70(3)$, obtained by analyzing the out-of-equilibrium dynamics when slowly crossing the transition point [59]. Although they appear slightly inconsistent with each other, they are both definitely larger than the relaxational dynamic exponent $z = 2.0245(15)$ of the 3D Ising model [61]. This substantial difference can be explained by recalling that the duality relation between the 3D \mathbb{Z}_2 gauge and standard Ising models is nonlocal. Therefore local relaxational upgradings may act differently, giving rise to different power laws associated with their respective critical slowing down.

To further investigate the out-of-equilibrium critical dynamics at the topological transition of the 3D lattice \mathbb{Z}_2 gauge model, we report numerical analyses of the critical relaxational flows [62] arising from instantaneous quenches to the critical point, starting from thermalized conditions within the critical region. Since the topological transition of the 3D \mathbb{Z}_2 gauge model does not

have local order parameters, the choice of the optimal observable to monitor the system during out-of-equilibrium evolutions is not straightforward. In this paper we focus on the simplest choice given by the local gauge-invariant energy density E , more precisely the subtracted energy density $E_s = E - E_c$ where E_c is the equilibrium energy density at the critical point. A crucial point of our approach is that, contrary to what happens at equilibrium, the time-dependent subtracted energy density E_s along the relaxational flows is not affected by the complications arising from the presence of analytical backgrounds at the transition point [62]. This is essentially due to the fact that the short-ranged modes responsible for the analytical background and the long-range critical modes have substantially different relaxational times around the critical point: the short-ranged modes are expected to thermalize much faster than the critical modes. This fact makes it possible to effectively isolate the out-of-equilibrium finite-size scaling (FSS) terms of the energy density, and therefore the power law of the critical time scale. As we shall see, this approach allows us to compute the dynamic exponent z , obtaining $z = 2.610(15)$, which significantly improves earlier results [58–60].

The paper is organized as follows. In Sec. II we introduce the 3D \mathbb{Z}_2 gauge model, summarizing its static critical properties, and present the dynamic protocol adopted to simulate the critical relaxational flows. In Sec. III we discuss the out-of-equilibrium behavior of the energy density along the critical relaxational flow within an out-of-equilibrium FSS framework. In Sec. IV we report our numerical analyses based on Monte Carlo (MC) simulations, leading to the estimate of the dynamic exponent z . Finally, in Sec. V we draw our conclusions.

II. CRITICAL RELAXATIONAL FLOW OF THE 3D \mathbb{Z}_2 GAUGE MODEL

A. The model

The 3D lattice \mathbb{Z}_2 gauge model [5] is a paradigmatic model undergoing a finite-temperature topological transition [2, 4]. Its Hamiltonian, defined on a cubic lattice, reads

$$H_G = -K \sum_{\mathbf{x}, \mu > \nu} \sigma_{\mathbf{x}, \mu} \sigma_{\mathbf{x} + \hat{\mu}, \nu} \sigma_{\mathbf{x} + \hat{\nu}, \mu} \sigma_{\mathbf{x}, \nu}, \quad (1)$$

where $\sigma_{\mathbf{x}, \mu} = \pm 1$ is the link variable associated with the bond starting from site \mathbf{x} in the positive μ direction, $\mu = 1, 2, 3$. The Hamiltonian parameter K plays the role of inverse gauge coupling, therefore the $K \rightarrow \infty$ limit corresponds to the small gauge-coupling limit. In the following we set the temperature $T = 1$, so that the partition function describing the equilibrium static properties reads

$$Z_G = \sum_{\{\sigma\}} e^{-H_G}. \quad (2)$$

In our numerical FSS analyses we will consider cubic-like systems of size L with periodic boundary conditions.

By a nonlocal duality relation [5, 10], the partition function Z_G in the infinite-volume limit can be exactly related to that of the standard cubic-lattice Ising model without external fields coupled to the spin variables, i.e.

$$Z_I = \sum_{\{s\}} e^{-H_I}, \quad H_I = -J \sum_{\mathbf{x}, \mu} s_{\mathbf{x}} s_{\mathbf{x} + \hat{\mu}}, \quad (3)$$

where $s_{\mathbf{x}, \mu} = \pm 1$ are spin variables associated with the sites \mathbf{x} of the cubic lattice, and the relation between J and K is

$$J = -\frac{1}{2} \ln \tanh K. \quad (4)$$

Notice that this duality mapping of the partition functions does not generally extend to finite-size systems with boundary conditions. In particular, it does not exactly relate the partition functions of \mathbb{Z}_2 gauge and Ising models when both of them have periodic boundary conditions [46], for which the equivalence is only recovered in the thermodynamic limit.

B. The finite-temperature topological transition

The 3D lattice \mathbb{Z}_2 gauge model undergoes a continuous transition separating a high- K deconfined phase from a low- K confined phase. Its transition point and static critical behavior can be obtained by exploiting the duality with the Ising model (3), for which accurate estimates of the critical point J_c are known, in particular, $J_c = 0.221654626(5)$ [63]. This allows us to obtain a corresponding accurate estimate of the critical point K_c of the 3D \mathbb{Z}_2 gauge model:

$$K_c = -\frac{1}{2} \ln \tanh J_c = 0.761413292(11). \quad (5)$$

The equivalence (up to analytical terms) of the partition functions of the 3D \mathbb{Z}_2 gauge and standard Ising models also implies that they share the same critical exponent ν related to the divergence of the correlation length, and also the leading scaling-correction exponent ω . In the following we use the Ising estimates [64] $\nu = 0.629971(4)$ for the length-scale critical exponent, $\alpha = 2 - 3\nu = 0.110087(12)$ for the specific-heat exponent, and $\omega = 0.8297(2)$ for the exponent associated with the leading scaling corrections (see also Refs. [63, 65–69]). As we shall see below, the analogy of the asymptotic critical behaviors of 3D \mathbb{Z}_2 gauge and Ising models does not extend to the critical dynamics, essentially because the highly nonlocal duality mapping [5, 10] does not extend to the local relaxational dynamics of both models.

One may also obtain accurate estimates of the energy density of the \mathbb{Z}_2 gauge model,

$$E = -\frac{1}{L^d} \left\langle \sum_{\mathbf{x}, \mu > \nu} \sigma_{\mathbf{x}, \mu} \sigma_{\mathbf{x} + \hat{\mu}, \nu} \sigma_{\mathbf{x} + \hat{\nu}, \mu} \sigma_{\mathbf{x}, \nu} \right\rangle, \quad (6)$$

by exploiting the duality mapping of the partition function Z_G to that of the 3D Ising model (3), for which accurate numerical results can be obtained by more effective MC algorithms, such as cluster algorithms [70]. In particular, one may compute the energy density

$$E_I = -\frac{1}{L^d} \left\langle \sum_{\mathbf{x}, \mu} s_{\mathbf{x}} s_{\mathbf{x}+\hat{\mu}} \right\rangle \quad (7)$$

of the 3D Ising model (3) at the critical point J_c . Then, by applying the duality mapping, one can determine the energy density E_c at the critical point K_c of the 3D \mathbb{Z}_2 gauge model, which we will use later in our analyses. For this purpose, we performed MC simulations of the Ising system (3) with periodic boundary conditions at the critical point J_c , for various lattice sizes up to $L = 300$, using mixtures of cluster and Metropolis algorithms. To obtain the critical infinite-volume energy density $E_{Ic} \equiv E_I(J_c, L \rightarrow \infty)$, these finite-size data are extrapolated by fitting them to the expected asymptotic large- L behavior $E_{Ic} + c L^{-(d-1/\nu)}$, see, e.g., Ref. [56] and also Eq. (12) below. This procedure allows us to obtain the accurate estimate $E_{Ic} = -0.990612(7)$ (this estimate is in agreement with, and significantly improves, earlier results, see, e.g., Refs. [71, 72]). Then, using the duality relation of the free-energy densities of the \mathbb{Z}_2 gauge and Ising models [5, 10],¹ we obtain the critical infinite-volume energy density of the 3D lattice \mathbb{Z}_2 gauge model with a relative accuracy of about 10^{-6} , i.e.,

$$E_c = -2.845971(3). \quad (10)$$

We finally mention that the area law of the Wilson loops W_C , defined as the product of the link variables along a closed contour C within a plane, provides a non-local order parameter for the topological transition of the 3D \mathbb{Z}_2 gauge model [5]. Indeed, their asymptotic large-size dependence changes at the transition point K_c : from the small- K area law $W_C \sim \exp(-c_a A_C)$ (where A_C is the area enclosed by the contour C and $c_a > 0$ is a constant) to the large- K perimeter law $W_C \sim \exp(-c_p P_C)$

¹ The relation between the free-energy densities F_G and F_I in the thermodynamic limit is given by [5, 10] (up to an irrelevant additive constant)

$$F_G(K) = -\frac{1}{L^d} \ln Z_G(K) = F_0(K) + F_I[J(K)], \quad (8)$$

$$F_0(K) = -\frac{3}{2} \ln \sinh(2K), \quad F_I(J) = -\frac{1}{L^d} \ln Z_I(J),$$

where $J(K)$ is given in Eq. (4). Then, the energy density of the 3D \mathbb{Z}_2 gauge model can be obtained by differentiating with respect to K ,

$$E = \frac{\partial F_G}{\partial K} = \frac{\partial F_0}{\partial K} + E_I[J(K)] \frac{\partial J(K)}{\partial K}, \quad (9)$$

where $E_I = \partial F_I / \partial J$. Finally, by evaluating it at $K = K_c$, using $J_c = J(K_c)$ and the Ising critical value $E_{Ic} \equiv E_I(J_c)$, one obtains Eq. (10).

(where P_C is the perimeter of the contour C and $c_p > 0$ is a constant).

C. Critical relaxational flow

To investigate the out-of-equilibrium critical dynamics at the topological transition, we consider *soft* quench protocols around the transition point [55, 73], so that the out-of-equilibrium evolution occurs within the critical region. In particular, we study the out-of-equilibrium critical relaxational flow arising from an instantaneous quench of the gauge parameter K , from $K < K_c$ to K_c . In practice, we consider the following protocol [62]:

(i) We start from a Gibbs ensemble of equilibrium configurations at $K < K_c$.

(ii) These configurations are the starting point for an out-of-equilibrium critical relaxational flow at the critical point K_c , parameterized by the dimensionless time t and starting at $t = 0$. This is achieved by making the system evolve using a purely local relaxational Metropolis dynamics at inverse coupling K_c [51, 57].

Since the dynamics is purely relaxational, the critical equilibrium of finite-size systems is eventually recovered for large times, which tend to be larger and larger with increasing L , due to the critical slowing down.

In our study we monitor the out-of-equilibrium dynamics arising from this quench protocol by the time dependence of the gauge-invariant energy density

$$E(t) = -\frac{1}{L^d} \left\langle \sum_{\mathbf{x}, \mu > \nu} \sigma_{\mathbf{x}, \mu} \sigma_{\mathbf{x}+\hat{\mu}, \nu} \sigma_{\mathbf{x}+\hat{\nu}, \mu} \sigma_{\mathbf{x}, \nu} \right\rangle_t, \quad (11)$$

defined as the average over the configurations obtained at a fixed time t along the relaxational flow. We do not consider nonlocal observables, like Wilson loops or Polyakov lines, whose analysis presents nontrivial drawbacks related to their complicated renormalizations arising from short-ranged fluctuations, see, e.g., Ref. [74], and also a significantly larger computational effort to obtain sufficiently accurate results.

It is worth mentioning that the critical relaxational flow at finite-temperature transitions is similar to the so-called gradient flow that is often exploited to numerically study the four-dimensional lattice quantum chromodynamics (QCD), which is the theory of strong interactions [75–78], in order to define a running coupling from the lattice energy density, see, e.g., Refs. [79–81]. Indeed, since the continuum limit of lattice QCD is realized in the zero-coupling (zero-temperature) limit, where the lattice length scale diverges exponentially, the critical (fixed-point) relaxational flow becomes a simple deterministic gradient flow at vanishing bare gauge coupling (corresponding to zero temperature), which is equivalent to a Langevin equation without stochastic term [50].

III. SCALING OF THE ENERGY DENSITY

In this section we analyze the out-of-equilibrium behavior of the energy density along the critical relaxational flow, associated with the quench protocol outlined in Sec. II C, within an out-of-equilibrium FSS framework. See Ref. [62] for more details.

A. Equilibrium finite-size scaling

In the absence of external symmetry-breaking fields, the equilibrium energy density E_e is expected to behave as [56]

$$E_e(K, L) \approx E_{\text{reg}}(r) + L^{-(d-y_r)} \mathcal{E}_e(\Upsilon), \quad (12)$$

where d is the dimension of the system, and

$$r \equiv K_c - K, \quad \Upsilon = r L^{y_r}, \quad y_r = 1/\nu. \quad (13)$$

The first contribution $E_{\text{reg}}(r)$ is a regular function of the deviation r from the critical point. The second scaling term represents the nonanalytic contribution from the critical modes, and the scaling function $\mathcal{E}_e(\Upsilon)$ is expected to be universal, apart from a multiplicative constant and a normalization of Υ . Note, however, that the scaling term turns out to be subleading with respect to the regular one, due to the fact that $d - y_r > 0$ at continuous transitions (if $y_r \geq d$ the singularity becomes inconsistent with a continuous transition). Therefore, the behavior of the energy density is dominated by the analytical background, which is associated with a mixing with the identity operator in the field-theoretical setting.

For later applications, it is useful to focus on the subtracted energy density

$$\begin{aligned} E_{se}(r, L) &\equiv E_e(r, L) - E_c, \\ E_c &\equiv E_e(r = 0, L \rightarrow \infty) = E_{\text{reg}}(0). \end{aligned} \quad (14)$$

Therefore $E_{se}(r = 0, L \rightarrow \infty) = 0$ by definition. A precise estimate of E_c has been already reported in Eq. (10). The scaling behavior of the subtracted energy density E_{se} is trivially obtained from Eq. (12),

$$\begin{aligned} E_{se}(r, L) &\approx \Delta E_{\text{reg}}(r) + L^{-(d-y_r)} \mathcal{E}_e(\Upsilon), \\ \Delta E_{\text{reg}}(r) &\equiv E_{\text{reg}}(r) - E_{\text{reg}}(0) = b_1 r + O(r^2), \end{aligned} \quad (15)$$

for generic systems (b_1 is a nonuniversal constant). Note that in the FSS limit, where $r \sim L^{-y_r}$, the regular term of the subtracted energy density $E_{se}(r, L)$ is subleading if

$$2y_r - d = \frac{2 - d\nu}{\nu} = \frac{\alpha}{\nu} > 0, \quad (16)$$

where α is the specific-heat exponent. This is the case of the 3D Ising universality class, where $\alpha \approx 0.110$. Therefore, for the 3D Ising models the contribution of

the regular term is subleading. However, it gives rise to very slowly decaying $O(L^{-\alpha/\nu})$ scaling corrections, with $\alpha/\nu \approx 0.1747$, which make the observation of the asymptotic equilibrium FSS of $E_{se}(r, L)$ a hard task in numerical analyses. As we shall see, this problem gets overcome along the critical relaxational flow, where the contributions from the regular term are suppressed, and the scaling corrections turn out to be $O(L^{-\omega})$ with $\omega \approx 0.83$.

B. Out-of-equilibrium finite-size scaling

To monitor the out-of-equilibrium behavior along the critical relaxational flow outlined in Sec. II C, we consider the subtracted post-quench energy density

$$E_s(t, r, L) \equiv E(t, r, L) - E_c, \quad (17)$$

where E_c is the equilibrium critical value of the energy density in the thermodynamic limit, cf. Eq. (10). Asymptotically, due to the large-time thermalization at the critical point (guaranteed by the relaxational flow for sufficiently large times at finite volume), E_s is suppressed as $E_s(t \rightarrow \infty) \sim L^{-(d-y_r)}$.

The out-of-equilibrium FSS of E_s can be obtained by extending the equilibrium FSS discussed in Sec. III A, adding a further dependence on the time scaling variable [55, 73, 82]

$$\Theta = t L^{-z}. \quad (18)$$

Therefore, the out-of-equilibrium FSS of the subtracted energy density E_s is expected to behave as [62]

$$\Omega(t, r, L) \equiv L^{d-y_r} E_s(t, r, L) \approx \mathcal{A}(\Theta, \Upsilon), \quad (19)$$

where \mathcal{A} is an out-of-equilibrium scaling function, which is expected to be universal apart from a multiplicative constant and trivial normalizations of the arguments.

Note that for Ising-like systems, the above asymptotic scaling behavior is expected to hold for any $\Theta \geq 0$. However, the scaling corrections are not uniform for $\Theta \rightarrow 0$. Indeed, as conjectured and numerically verified in Ref. [62] (see also Ref. [83] for similar results within quantum transitions and the unitary quantum dynamics), the contribution of the regular term to the subtracted energy density gets rapidly suppressed along the critical relaxational flow. This is related to the fact that the effective thermalization of the short-ranged modes that give rise to the regular background of the energy density, cf. Eq. (12), requires a much shorter time scale τ_B than the critical modes, i.e., $\tau_B \ll \tau \sim L^z$, so that their asymptotic equilibrium contribution E_c is effectively approached instantaneously in terms of the rescaled time variable $\Theta = t/L^z$ [62]. Thus the residual $O(L^{-n\alpha/\nu})$ equilibrium contributions ($n \geq 1$ is an integer number), arising from the expansion of the regular term in powers of r , cf. Eq. (15), are expected to disappear from the asymptotic out-of-equilibrium FSS of the subtracted

energy density at any $\Theta > 0$. Therefore the scaling corrections are expected to be $O(L^{-\omega})$ for any fixed $\Theta > 0$, with $\omega \approx 0.83$ significantly larger than $\alpha/\nu \approx 0.17$. This scenario will be further confirmed by the numerical analyses presented in the next section. This is a crucial point for the effectiveness of our approach based on the analysis of the subtracted energy density along the relaxational flow, and, in particular, to obtain an accurate estimate of the dynamic exponent z .

However, assuming that the limit $\Theta \rightarrow 0$ matches with the time dependence of the subtracted energy density (which must be smooth in finite-size systems), the disappearance of the $O(L^{-\alpha/\nu})$ scaling corrections from the asymptotic behaviors at fixed $\Theta > 0$ must reemerge as a nonanalytical behavior of the scaling function $\mathcal{A}(\Theta, \Upsilon)$ in the $\Theta \rightarrow 0$ limit, i.e., [62]

$$\mathcal{A}(\Theta, \Upsilon) \approx f_0(\Upsilon) + f_1(\Upsilon) \Theta^{\alpha/\nu}. \quad (20)$$

In conclusion, for $\Theta > 0$ we generally expect

$$\begin{aligned} \Omega(t, r, L) &= \mathcal{A}(\Theta, \Upsilon) + \\ &+ L^{-\omega} \mathcal{A}_\omega(\Theta, \Upsilon) + \dots + L^{-\omega_2} \mathcal{A}_{\omega_2}(\Theta, \Upsilon) + \dots \end{aligned} \quad (21)$$

where the dots indicate more suppressed terms, such as $O(L^{-n\omega})$ with $n > 1$, and corrections from other irrelevant RG perturbations. The subleading scaling corrections associated with $\omega_2 \approx 2.02$ arise from the breaking of the rotational invariance in cubic-lattice systems [65, 84, 85].

We finally note that the subtraction of the critical energy density E_c can be avoided by evaluating the derivative of the energy density along the relaxational flow. Indeed, by taking the time derivative of $\Omega(t, r, L)$ defined in Eq. (19), we obtain the relation

$$\begin{aligned} L^z \frac{d\Omega(t, r, L)}{dt} &= L^{d-y_r+z} \frac{dE(t, r, L)}{dt} \\ &\approx \frac{\partial \mathcal{A}(\Theta, \Upsilon)}{\partial \Theta} = \mathcal{A}_t(\Theta, \Upsilon), \end{aligned} \quad (22)$$

where \mathcal{A}_t is another scaling function whose computation does not require the knowledge of E_c .

IV. NUMERICAL RESULTS

In this section we present our numerical analyses of the out-of-equilibrium behavior of the subtracted energy density $E_s(t, r, L)$, cf. Eq. (17), along the critical relaxational flow driven by standard single-spin-flip Metropolis upgradings: the transition probability for a flip of the link variable $\sigma_{\mathbf{x}, \mu}$ is given by

$$P(\sigma_{\mathbf{x}, \mu} \rightarrow -\sigma_{\mathbf{x}, \mu}) = \text{Min}[1, e^{-\Delta H_G}], \quad (23)$$

where ΔH_G is the variation of the lattice Hamiltonian (1) when replacing $\sigma_{\mathbf{x}, \mu} \rightarrow -\sigma_{\mathbf{x}, \mu}$. One MC time unit corresponds to a global sweep of a single Metropolis upgrading

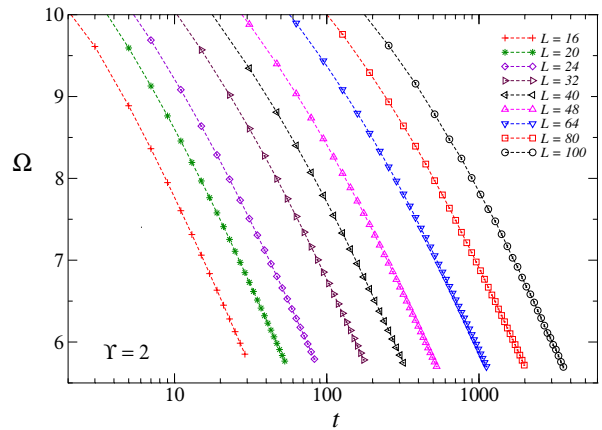


FIG. 1: Data of $\Omega \equiv E_s L^{d-y_r}$ versus the MC time t for various lattice sizes up to $L = 100$, keeping $\Upsilon = 2$ fixed (note that we use a logarithmic scale for the time axis). The statistical errors of the data are very small and hardly visible.

proposal for each bond variable (we use a checkerboard upgrading scheme, where we separately upgrade link variables along a given direction at odd and even sites). Its acceptance ratio turns out to be relatively small at the critical point K_c , about 2% [note that this acceptance ratio is much smaller than that of the analogous Metropolis upgrading at the critical point J_c of the Ising model (3), which is about 50%]. We consider cubic-like systems of size L and volume $V = L^3$, with periodic boundary conditions.

We present results for the critical relaxational flow of the 3D \mathbb{Z}_2 gauge model at some fixed values of Υ , i.e., $\Upsilon = 2, 4, 8$, up to lattice sizes $L = 100$ (more precisely for $L = 16, 20, 24, 32, 40, 48, 64, 80, 100$), obtained by averaging the time-dependent energy density defined in Eq. (11), over a large number of trajectories implementing the critical relaxational flow. In practice, along the equilibrium run at $K < K_c$, corresponding to a given value of Υ , we start a trajectory every $n \approx 0.2 L^z$ sweeps at equilibrium, where we used the preliminary value $z = 2.6$ (this distance between trajectories provides a reasonable compromise to get almost decorrelated starting configurations, as checked by preliminary tests). We collect about $O(10^6)$ relaxational trajectories for $L \leq 80$, and about 2.5×10^5 trajectories for the largest lattice size $L = 100$. Any trajectory typically runs up to $t \approx 0.02 L^z$, thus increasing its duration when increasing L , to obtain averages at fixed $\Theta = t/L^z$ up to $\Theta \approx 0.02$. Therefore the numerical effort per trajectory increases as L^{3+z} with increasing L . The error on the average of the energy density over the trajectories is estimated by a blocking procedure to properly take into account the residual autocorrelations among the sequential trajectories along the equilibrium run. The large number of trajectories allows us to estimate the average energy density along the critical relaxational flow with high accuracy, for example with a relative accuracy of about 2×10^{-6} for $L = 100$.

In Fig. 1 we show some raw data of the subtracted en-

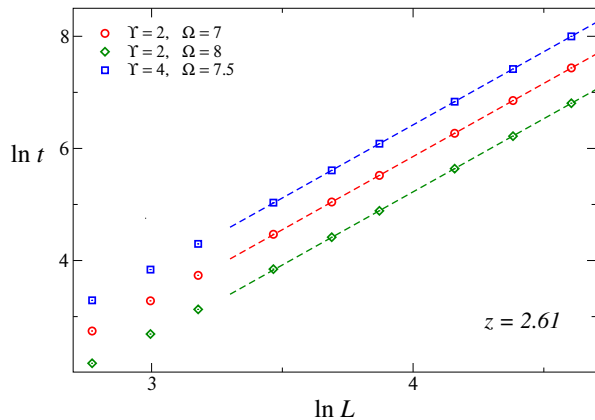


FIG. 2: Some data of the time versus the lattice size, computed at fixed Υ and Ω , in logarithmic scale. The lines show linear fits of the data for $L \geq 40$ with $z = 2.61$ (with $\chi^2/\text{d.o.f} \lesssim 1$). The statistical errors of the data are hardly visible in these plots.

ergy density E_s , in particular $\Omega = E_s L^{d-y_r}$, versus the time t , for various values of L at fixed $\Upsilon = rL^{y_r} = 2$. As we shall see, the analysis of these data within the out-of-equilibrium FSS framework outlined in Sec. III allows us to estimate the dynamic exponent z associated with the purely relaxational dynamics, by determining the optimal collapse of the data when plotting them versus $\Theta = tL^{-z}$.

Since the data along the critical relaxational flow are highly correlated, we must pay some attention to extract a reliable estimate of the power law controlling the time dependence. For this purpose, it is convenient to consider the time $t(\Omega)$ as a function of the rescaled subtracted energy density Ω (this is well defined because Ω is a monotonic function of t along the critical relaxational flow). Numerically, this can be easily estimated by linearly interpolating the data of $\Omega(t, r, L)$ as a function of t (one may also use higher-order interpolations), using a straightforward propagation of the statistical error. One can easily derive the corresponding out-of-equilibrium FSS from that of the subtracted energy density, cf. Eq. (21), obtaining

$$t(\Omega, r, L) \approx L^z F(\Omega, \Upsilon) + L^{z-\omega} F_\omega(\Omega, \Upsilon) + \dots + L^{z-\omega_2} F_{\omega_2}(\Omega, \Upsilon) + \dots \quad (24)$$

In our analyses we also consider the difference

$$\Delta t(\Omega, r_2, r_1, L) \equiv t(\Omega, r_2, L) - t(\Omega, r_1, L) \approx L^z F_d(\Omega, \Upsilon_2, \Upsilon_1), \quad (25)$$

where $\Upsilon_i = r_i L^{y_r}$, because we noted that these differences are less affected by scaling corrections.

To avoid the problems of the statistical correlations among the data for different values of Ω , we perform fits of the data of $t(\Omega, r, L)$ at fixed values of Υ and Ω , so that the data considered are statistically independent.

We consider, and compare the results, of fits to various ansatz functions, such as

$$(a): t(\Omega, \Upsilon, L) = a_0 L^z, \quad (26)$$

$$(b): t(\Omega, \Upsilon, L) = a_0 L^z (1 + a_1 L^{-\omega}), \quad (27)$$

$$(c): t(\Omega, \Upsilon, L) = a_0 L^z (1 + a_1 L^{-\omega} + a_2 L^{-2}). \quad (28)$$

Of course, the coefficients a_i of the above asymptotic behaviors depend on Υ and Ω . The fit (c) is also useful because for the smallest lattice sizes the scaling corrections are apparently dominated by contributions approximately decaying as $O(L^{-2})$, which may, for example, be associated with the next-to-leading irrelevant RG perturbations associated with the lattice anisotropy, cf. Eq. (21). In Table I, we report the results of some of the above fits, at some values of Ω that turn out to be optimal. For example, the region $\Omega \approx 7$ provides the most stable fits for $\Upsilon = 2$, corresponding to $\Theta = t/L^z \approx 0.01$. Fig. 2 shows some data of the time $t(\Omega, \Upsilon, L)$ for some values of Ω and Υ , with their best fits, to highlight the accuracy of the estimate of z . We also note that the results are subject to larger scaling corrections at larger values of Ω , corresponding to smaller values of Θ , and provide substantially consistent, but less accurate, results. This is easily explained by the expected crossover behavior of the scaling corrections in the limit $\Theta \rightarrow 0$, where they are expected to pass from $O(L^{-\omega})$ at $\Theta > 0$ to $O(L^{-\alpha/\nu})$ for $\Theta = 0$.

On the basis of the results obtained by the various fits, see in particular Table I, we report

$$z = 2.610(15) \quad (29)$$

as our final estimate, where the error takes into account the range of results obtained by the different fits considered, and also the variation due to uncertainty on the available estimates of K_c and E_c , cf. Eqs. (5) and (10) respectively, which are much smaller. The quality of the resulting scaling behavior within the whole critical relaxational flow can be appreciated looking at the plots shown in Fig. 3, where we report $\Omega(t, r, L)$ versus Θ using the estimate (29): the asymptotic collapse of the curves for any $\Theta > 0$ is clearly observed. It is also worth mentioning that consistent, although less precise, results are obtained by looking for the optimal collapse of the data of the time derivative of Ω , cf. Eq. (22), which does not require the knowledge of E_c .

We also note that the behavior for small Θ confirms the $\Theta \rightarrow 0$ nonanalyticity (20) of the scaling function $\mathcal{A}(\Theta, \Upsilon)$, see Fig. 4 where data for $\Upsilon = 2$ and $\Upsilon = 4$ are shown. Note also that the data at $t = 0$, or $\Theta = 0$, show clearly a different approach to the asymptotic FSS limit with respect to the data at $\Theta > 0$. Indeed, while at $t = 0$ the equilibrium FSS is approached from below, at fixed $\Theta > 0$ the out-of-equilibrium FSS is approached from above, see, e.g., the plots reported in Fig. 5. This is in agreement with the fact that the leading $O(L^{-\alpha/\nu})$ scaling corrections arising from the regular term at equilibrium (also corresponding to the so-called mixing with

	Ω	Ansatz	L_{\min}	z	$\chi^2/\text{d.o.f.}$
$\Upsilon = 2$	6	(a)	40	2.613(1)	0.9
			48	2.613(2)	1.3
	7	(a)	40	2.610(2)	0.5
			48	2.611(2)	0.3
		(b)	40	2.617(15)	0.6
			(c)	16	2.589(10)
		20	2.591(15)	0.4	
		24	2.594(24)	0.4	
8	(a)	40	2.607(2)	2.5	
		48	2.612(3)	0.8	
$\Upsilon = 4$	7.5	(a)	40	2.608(1)	0.4
			48	2.608(1)	0.4
	(c)	16	2.611(5)	1.2	
	20	2.613(8)	1.3		
D_{24}	7.5	(a)	32	2.603(1)	1.0
			40	2.606(2)	0.4
			48	2.605(3)	0.3
	(c)	16	2.598(13)	0.4	
	20	2.600(20)	0.4		
D_{48}	8	(a)	48	2.592(6)	1.5
			64	2.600(11)	1.6
C_{24}	7.5	(a)	40	2.608(1)	0.8
			48	2.609(1)	0.7
			64	2.610(2)	0.3
	(b)	40	2.618(8)	0.5	
	48	2.616(13)	0.4		
C_{248}	8	(a)	48	2.610(1)	4.9
			64	2.613(1)	2.8

TABLE I: Some results of fits of the data of $t(\Omega, r, L)$ at fixed values of Ω , cf. Eq. (24) for $\Upsilon = 2$, $\Upsilon = 4$, the difference between the data for different Υ at fixed Ω (denoted by D_{24} and D_{48}), and the combined fit of the data for $\Upsilon = 2$, $\Upsilon = 4$ (denoted by C_{24}) and those for $\Upsilon = 2, 4, 8$ (denoted by C_{248}). We report results for fits of type (a), (b), and (c) defined in Eqs. (26)-(28). The values of Ω chosen for the fits correspond to the optimal region $\Theta = t/L^z \approx 0.01$, where scaling corrections turn out to be smaller. On the basis of these results, we arrive at $z = 2.610(15)$ as our final estimate, where the error takes into account the small differences of the results, including most results reported in the table (the error is essentially dominated by the differences of the various fits, while statistical errors are generally much smaller). Other fits for different values of Ω give consistent, but less precise, results.

the identity operator in the field-theoretical language), cf. Eq. (15), get suppressed along the critical relaxational flow, whose asymptotic approach is expected to be characterized by more standard $O(L^{-\omega})$ decaying corrections [62, 83].

We finally mention that the out-of-equilibrium estimate (29) improves earlier results obtained by other approaches, reported in Refs. [58–60]. In particular, it is in

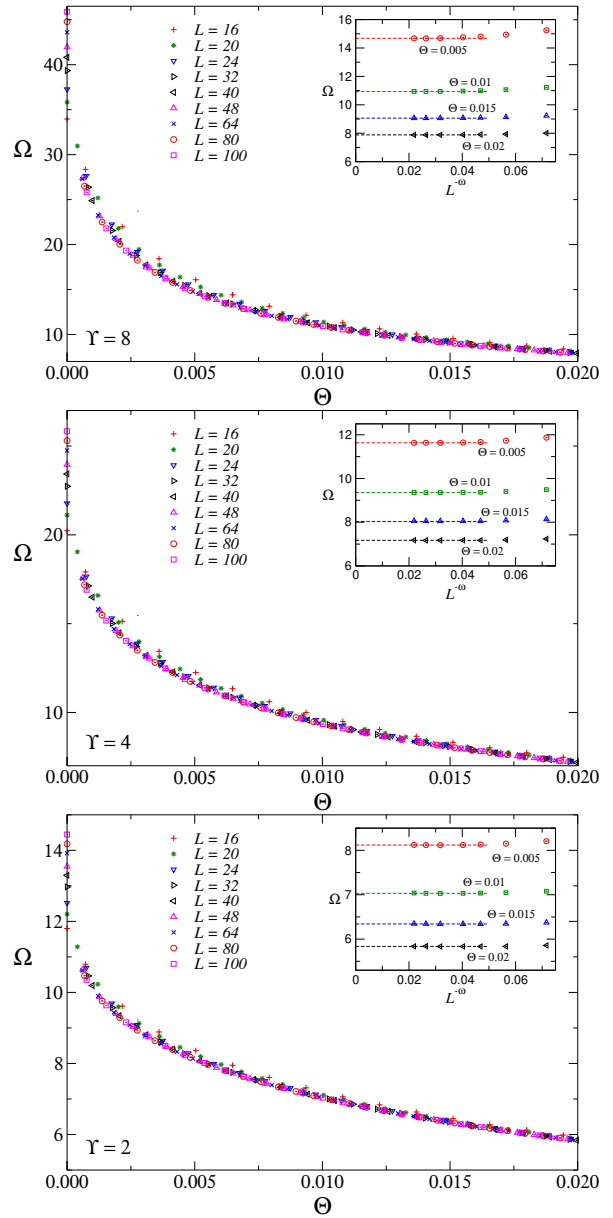


FIG. 3: We plot $\Omega \equiv E_s L^{d-y_r}$ versus $\Theta = t/L^z$ using our optimal estimate $z = 2.61$, for $\Upsilon = 2$ (bottom), $\Upsilon = 4$ (middle), and $\Upsilon = 8$ (top). The insets show the convergence to the asymptotic scaling behavior for some values of Θ , plotting the data of Ω versus $L^{-\omega}$ which is the expected rate of convergence, while the dashed lines represent the asymptotic value $\mathcal{A}(\Theta, \Upsilon)$.

agreement with the result $z = 2.55(6)$ obtained analyzing the equilibrium critical dynamics [60]. We also note that our new result maintains the apparent small discrepancy with the estimate $z = 2.70(3)$ obtained in Ref. [59] by analyzing the out-of-equilibrium behavior of the Polyakov lines when slowly changing the temperature to cross the transition point.

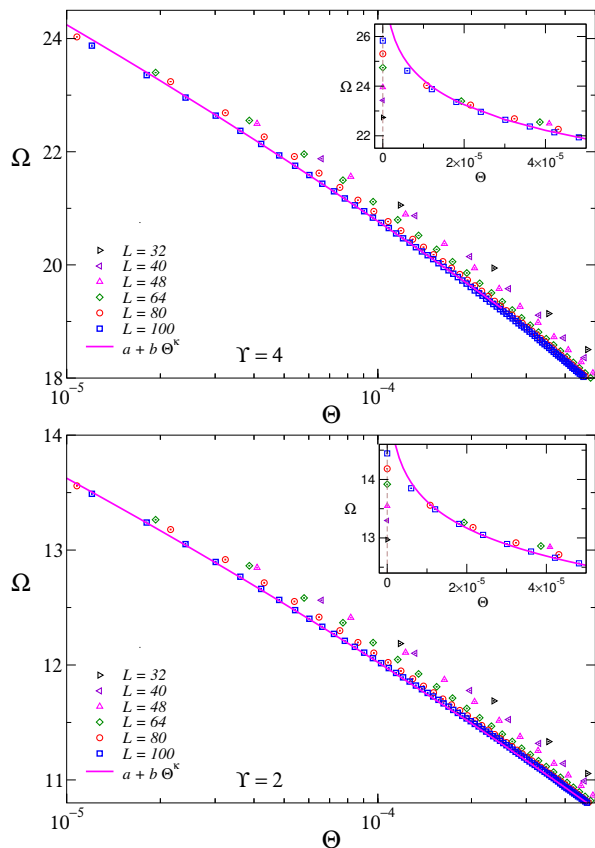


FIG. 4: We show data of $\Omega(t, r, L)$ for small values of $\Theta = t/L^z$ using our optimal estimate $z = 2.61$, at fixed $\Upsilon = 2$ (bottom) and $\Upsilon = 4$ (top). The data support the expected behavior (20). This is shown by the full line, corresponding to a fit of the $L = 100$ data in the range $3 \times 10^{-5} \lesssim \Theta \lesssim 3 \times 10^{-4}$ to $a + b\Theta^\kappa$ with $\kappa = \alpha/(\nu z) \approx 0.0669$ (we prefer to show this fit assuming $L = 100$ large enough, instead of extrapolating the data to $L \rightarrow \infty$, which requires a quite cumbersome procedure in the small- Θ crossover region $\Theta \lesssim 10^{-4}$). The insets show the same data close to $\Theta = 0$ without logarithmic scale (the vertical dashed lines indicate the $\Theta = 0$ starting point of the relaxational flow), to highlight the crossover from the equilibrium behavior at $t = 0$ to the out-of-equilibrium scaling behavior at small values of Θ .

V. CONCLUSIONS

We have studied the out-of-equilibrium critical dynamics of 3D lattice \mathbb{Z}_2 gauge models, along critical relaxational flows arising from instantaneous quenches to the critical point, driven by purely relaxational local Metropolis upgradings of the link \mathbb{Z}_2 gauge variables. We monitor the critical dynamics by computing the local energy density, which is the simplest gauge-invariant quantity that can be computed in a lattice gauge theory. We analyze the behavior along the critical relaxational flow within an out-of-equilibrium FSS framework, exploiting the suppression of the regular contributions that generally affect the equilibrium free-energy density and the energy density at the critical point [62].

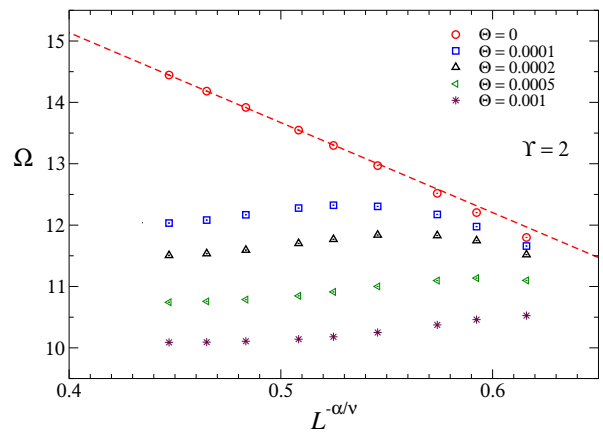


FIG. 5: We show data of $\Omega(t, r, L)$ for some values of $\Theta = t/L^z$, from $\Theta = 0$ to $\Theta = 0.01$, using our optimal estimate $z = 2.61$, at fixed $\Upsilon = 2$. They are plotted versus $L^{-\alpha/\nu}$ which is the expected rate of suppression of the leading scaling corrections at $t = \Theta = 0$, as confirmed by the almost linear behavior of the equilibrium data for $\Theta = 0$ (the dashed line shows a linear fit of the equilibrium $t = 0$ data for the largest lattice sizes with $L \geq 48$ to $a + bL^{-\alpha/\nu}$). Note also the substantially different behavior of the scaling corrections for $\Theta > 0$ along the critical relaxational flow, where the data confirm that the $O(L^{-\alpha/\nu})$ corrections vanish at fixed $\Theta > 0$, leaving only more suppressed $O(L^{-\omega})$ corrections.

By matching the numerical data up to relatively large lattice sizes with the scaling behavior predicted by the out-of-equilibrium FSS theory outlined in Sec. III B, we obtain the estimate $z = 2.610(15)$ for the dynamic exponent associated with the local purely relaxational dynamics of the 3D \mathbb{Z}_2 gauge universality class. This result significantly improves earlier computations of the dynamic exponent z , see Refs. [58–60], obtained by both equilibrium and out-equilibrium studies. In particular, our estimate of z is in agreement with the result $z = 2.55(6)$ obtained by analyzing the equilibrium critical dynamics [60].

Our results confirm that the critical slowing down experienced by the lattice \mathbb{Z}_2 gauge models is stronger than that associated with the relaxational dynamics of the standard Ising universality class, whose dynamic exponent $z = 2.0245(15)$ [61] is significantly smaller. This difference can be explained by noting that the duality relation between the \mathbb{Z}_2 gauge and Ising universality classes is nonlocal. Therefore local relaxational upgradings act on substantially different modes, giving rise to different critical relaxational dynamics, and therefore different values of the dynamic exponents controlling the power law of the critical slowing down.

We finally remark that the out-of-equilibrium method exploited in this study, based on the study of the critical relaxational flow of the local gauge-invariant energy density, is expected to be effective to address the critical dynamics of any system with gauge symmetries, whose critical modes at their topological transition can be hardly

monitored due to the absence of a local order parameter. For example, one interesting case is the 3D lattice Abelian Higgs model with a one-component complex scalar field, whose continuous transitions do not have any local order parameter, analogously to the 3D \mathbb{Z}_2 gauge model, see, e.g., Refs. [2, 46, 48].

Acknowledgments

H.P. thanks the University of Pisa for the kind hospitality. H.P. would like to acknowledge support from

the project CONCEPT/0823/0052, implemented under the program “THALIA 2021-2027” and co-funded by the European Union through the Cyprus Research and Innovation Foundation (RIF). C.B. and E.V. acknowledge support from project PRIN 2022 “Emerging gauge theories: critical properties and quantum dynamics” (20227JZKWP).

-
- [1] S. Sachdev, *Quantum Phases of Matter*, Cambridge University Press, Cambridge, 2023.
- [2] C. Bonati, A. Pelissetto, and E. Vicari, Three-dimensional Abelian and non-Abelian gauge Higgs theories, arXiv:2410.05823.
- [3] T. Senthil, Deconfined quantum critical points: a review, in *50 years of the renormalization group*, dedicated to the memory of Michael E. Fisher, edited by Amnon Aharony, Ora Entin-Wohlman, David Huse, and Leo Radzihovsky, World Scientific arXiv:2306.12638.
- [4] S. Sachdev, Topological order, emergent gauge fields, and Fermi surface reconstruction, *Rep. Prog. Phys.* **82**, 014001 (2019).
- [5] F. J. Wegner, Duality in generalized Ising models and phase transitions without local order parameters, *Jour. of Math. Phys.* **12**, 2259 (1971).
- [6] R. Balian, J. M. Drouffe, and C. Itzykson, Gauge fields on a lattice. i. general outlook, *Phys. Rev. D* **10**, 3376 (1974); Gauge fields on a lattice. II. Gauge-invariant Ising model, *Phys. Rev. D* **11**, 2098 (1975).
- [7] K. Osterwalder and E. Seiler, Gauge Field Theories on the Lattice, *Ann. Phys. (NY)* **110**, 440 (1978).
- [8] E. Fradkin and S. Shenker, Phase diagrams of lattice gauge theories with Higgs fields, *Phys. Rev. D* **19**, 3682 (1979).
- [9] J. B. Kogut, An introduction to lattice gauge theory and spin systems, *Rev. Mod. Phys.* **51**, 659 (1979).
- [10] R. Savit, Duality in Field Theory and Statistical Systems, *Rev. Mod. Phys.* **52**, 453 (1980).
- [11] C. Dasgupta and B. I. Halperin, Phase Transitions in a Lattice Model of Superconductivity, *Phys. Rev. Lett.* **47**, 1556 (1981).
- [12] K. Fredenhagen and M. Marcu, Charged states in \mathbb{Z}_2 gauge theories, *Commun. Math. Phys.* **92**, 81 (1983).
- [13] T. Kennedy and C. King, Symmetry Breaking in the Lattice Abelian Higgs Model, *Phys. Rev. Lett.* **55**, 776 (1985).
- [14] T. Kennedy and C. King, Spontaneous Symmetry Breakdown in the Abelian Higgs Model, *Commun. Math. Phys.* **104**, 327 (1986).
- [15] C. Borgs and F. Nill, The Phase Diagram of the Abelian Lattice Higgs Model. A Review of Rigorous Results, *J. Stat. Phys.* **47**, 877 (1987)
- [16] G. Murthy and S. Sachdev, Actions of hedgehogs instantons in the disordered phase of 2+1 dimensional CP^{N-1} model, *Nucl. Phys. B* **344**, 557 (1990).
- [17] P. E. Lammert, D. D. Roskar, and J. Toner, Topology and nematic ordering, *Phys. Rev. Lett.* **70**, 1650 (1993); Topology and nematic ordering. I. A gauge theory, *Phys. Rev. E* **52**, 1778 (1995); Topology and nematic ordering. II. Observable critical behavior, *Phys. Rev. E* **52**, 1801 (1995).
- [18] M. Kiometzis, H. Kleinert, and A. M. J. Schakel, Critical Exponents of the Superconducting Phase Transition, *Phys. Rev. Lett.* **73**, 1975 (1994).
- [19] F. Herbut and Z. Tesanovic, Critical Fluctuations in Superconductors and the Magnetic Field Penetration Depth, *Phys. Rev. Lett.* **76**, 4588 (1996).
- [20] V. Yu. Irkhin, A. A. Katanin, and M. I. Katsnelson, $1/N$ expansion for critical exponents of magnetic phase transitions in the CP^{N-1} model for $2 < d < 4$, *Phys. Rev. B* **54**, 11953 (1996).
- [21] K. Kajantie, M. Karjalainen, M. Laine, and J. Peisa, Masses and phase structure in the Ginzburg-Landau model, *Phys. Rev. B* **57**, 3011 (1998).
- [22] T. Senthil and M. P. A. Fisher, \mathbb{Z}_2 gauge theory of electron fractionalization in strongly correlated systems, *Phys. Rev. B* **62**, 7850 (2000).
- [23] R. D. Sedgewick, D. J. Scalapino, and R. L. Sugar, Fractionalized phase in an $XY - \mathbb{Z}_2$ gauge model, *Phys. Rev. B* **65**, 054508 (2002).
- [24] A. Sudbø, E. Smørgrav, J. Smiseth, F. S. Nogueira, and J. Hove, Criticality in the (2+1)-Dimensional Compact Higgs Model and Fractionalized Insulators, *Phys. Rev. Lett.* **89**, 226403 (2002).
- [25] H. Kleinert, F. S. Nogueira, and A. Sudbø, Deconfinement Transition in Three-Dimensional Compact $U(1)$ Gauge Theories Coupled to Matter Fields, *Phys. Rev. Lett.* **88**, 232001 (2002).
- [26] S. Mo, J. Hove, and A. Sudbø, Order of the metal-to-superconductor transition, *Phys. Rev. B* **65**, 104501 (2002).
- [27] T. Senthil and O. Motrunich, Microscopic models for fractionalized phases in strongly correlated systems, *Phys. Rev. B* **66**, 205104 (2002).
- [28] T. Neuhaus, A. Rajantie, and K. Rummukainen, Numerical study of duality and universality in a frozen superconductor, *Phys. Rev. B* **67**, 014525 (2003).
- [29] J. Smiseth, E. Smørgrav, F. S. Nogueira, J. Hove, and A. Sudbø, Phase Structure of $d = 2 + 1$ Compact Lattice Gauge Theories and the Transition from Mott Insulator to Fractionalized Insulator, *Phys. Rev. B* **67**, 205104 (2003).

- (2003).
- [30] R. K. Kaul and S. Sachdev, Quantum criticality of U(1) gauge theories with fermionic and bosonic matter in two spatial dimensions, *Phys. Rev. B* **77**, 155105 (2008).
- [31] D. Charrier, F. Alet, and P. Pujol, Gauge Theory Picture of an Ordering Transition in a Dimer Model, *Phys. Rev. Lett.* **101**, 167205 (2008)
- [32] K. Liu, J. Nissinen, Z. Nussinov, R.-J. Slager, K. Wu, and J. Zaanen, Classification of nematic order in 2+1 dimensions: Dislocations melting and $O(2)/Z_N$ lattice gauge theory, *Phys. Rev. B* **91**, 075103 (2015).
- [33] A. Nahum, J. T. Chalker, P. Serna, M. Ortuño, and A. M. Somoza, Deconfined Quantum Criticality, Scaling Violations, and Classical Loop Models, *Phys. Rev. X* **5**, 041048 (2015).
- [34] C. Bonati, A. Pelissetto, and E. Vicari, Higher-charge three-dimensional compact lattice Abelian-Higgs models, *Phys. Rev. E* **102**, 062151 (2020).
- [35] C. Bonati, A. Pelissetto, and E. Vicari, Lattice Abelian-Higgs model with noncompact gauge fields, *Phys. Rev. B* **103**, 085104 (2021).
- [36] A. Somoza, P. Serna, and A. Nahum, Self-dual criticality in three-dimensional Z_2 gauge theory with matter, *Phys. Rev. X* **11**, 041008 (2021).
- [37] C. Bonati, A. Pelissetto, and E. Vicari, Critical behaviors of lattice U(1) gauge models and three-dimensional Abelian-Higgs gauge field theory, *Phys. Rev. B* **105**, 085112 (2022).
- [38] C. Bonati, A. Pelissetto, and E. Vicari, Multicritical point of the three-dimensional Z_2 gauge Higgs model, *Phys. Rev. B* **105**, 165138 (2022).
- [39] G. Bracci-Testasecca and A. Pelissetto, Multicomponent gauge-Higgs models with discrete Abelian gauge groups, *J. Stat. Mech.* **04**, 043101 (2023).
- [40] C. Bonati and N. Francini, Noncompact lattice Higgs model with Abelian discrete gauge groups: Phase diagram and gauge symmetry enlargement, *Phys. Rev. B* **107**, 035106 (2023).
- [41] Y.-H. Zhang, Z. Zhu, and A. Vishwanath, XY^* transition and extraordinary boundary criticality from fractional exciton condensation in quantum hall bilayer, *Phys. Rev. X* **13**, 031023 (2023).
- [42] C. Bonati, A. Pelissetto, and E. Vicari, Coulomb-Higgs phase transition of three-dimensional lattice Abelian Higgs gauge models with noncompact gauge variables and gauge fixing *Phys. Rev. E* **108**, 044125 (2023).
- [43] C. Bonati, A. Pelissetto, and E. Vicari, Three-dimensional Z_2 -gauge N -vector models, *Phys. Rev. B* **109**, 235121 (2024).
- [44] C. Bonati, A. Pelissetto, and E. Vicari, Uncovering critical vector order-parameter correlations by a stochastic gauge fixing at $O(N)^*$ and Ising* continuous transitions, *Phys. Rev. B* **110**, 125109 (2024).
- [45] W.-T. Xu, F. Pollmann, and M. Knap, Critical behavior of the Fredenhagen-Marcu order parameter at topological phase transitions, arXiv:2402.00127.
- [46] C. Bonati, A. Pelissetto, and E. Vicari, Deconfinement transitions in three-dimensional compact lattice Abelian Higgs models with multiple-charge scalar fields, *Phys. Rev. E* **109**, 044146 (2024).
- [47] P. Serna, A. M. Somoza, and A. Nahum, Worldsheet patching, 1-form symmetries, and “Landau-star” phase transitions, arXiv:2403.04025.
- [48] C. Bonati, A. Pelissetto, and E. Vicari, Diverse universality classes of the topological deconfinement transitions of three-dimensional noncompact lattice Abelian-Higgs models, *Phys. Rev. D* **109**, 034517 (2024).
- [49] C. Bonati, A. Pelissetto, I. Soler Calero, and E. Vicari, Charged critical behavior and nonperturbative continuum limit of three-dimensional lattice $SU(N_c)$ gauge Higgs models, *Phys. Rev. D* **110**, 094504 (2024).
- [50] S.-k. Ma, *Modern theory of critical phenomena*, Routledge Editor (New York, 2001).
- [51] P. C. Hohenberg and B. I. Halperin, Theory of dynamic critical phenomena, *Rev. Mod. Phys.* **49**, 435 (1977).
- [52] P. Calabrese and A. Gambassi, Ageing Properties of Critical Systems, *J. Phys. A* **38**, R133 (2005).
- [53] R. Folk and G. Moser, Critical dynamics: A field-theoretical approach, *J. Phys. A: Math. Gen.* **39**, R207 (2006).
- [54] A. Chandran, A. Erez, S. S. Gubser, and S. L. Sondhi, Kibble-Zurek problem: Universality and the scaling limit, *Phys. Rev. B* **86**, 064304 (2012).
- [55] D. Rossini and E. Vicari, Coherent and dissipative dynamics at quantum phase transitions, *Phys. Rep.* **936**, 1 (2021).
- [56] A. Pelissetto and E. Vicari, Critical phenomena and renormalization group theory, *Phys. Rep.* **368**, 549 (2002).
- [57] K. Binder, Monte Carlo investigations of phase transitions and critical phenomena. *Phase Transitions and Critical Phenomena*, Domb, C. & Green, M. S. (eds.) vol. 5b, 1 (Academic Press, London, 1976).
- [58] R. Ben-Av, D. Kandel, E. Katznelson, P. G. Lauwers, and S. Solomon, Critical acceleration of lattice gauge simulations. *Journal of Stat. Phys.* **58**, 125 (1990).
- [59] N. Xu, C. Castelnovo, R. G. Melko, C. Chamon, and A. W. Sandvik, Dynamic scaling of topological ordering in classical systems, *Phys. Rev. B* **97**, 024432 (2018).
- [60] C. Bonati, A. Pelissetto, and E. Vicari, Critical relaxational dynamics at the continuous transitions of three-dimensional spin models with Z_2 gauge symmetry, arXiv:2501.09575.
- [61] M. Hasenbusch, The dynamic critical exponent z of the three-dimensional Ising universality class: Monte Carlo simulations of the improved Blume-Capel model, *Phys. Rev. E* **101**, 022126 (2020).
- [62] H. Panagopoulos and E. Vicari, Out-of-equilibrium scaling of the energy density along the critical relaxational flow after a quench of the temperature, *Phys. Rev. E* **109**, 064107 (2024).
- [63] A. M. Ferrenberg, J. Xu, and D. P. Landau, Pushing the limits of Monte Carlo simulations for the three-dimensional Ising model, *Phys. Rev. E* **97**, 043301 (2018).
- [64] F. Kos, D. Poland, D. Simmons-Duffin, and A. Vichi, Precision islands in the Ising and $O(N)$ models, *JHEP* **08**, 036 (2016).
- [65] M. Hasenbusch, Restoring isotropy in a three-dimensional lattice model: The Ising universality class, *Phys. Rev. B* **104**, 014426 (2021).
- [66] M. Hasenbusch, A finite size scaling study of lattice models in the three-dimensional Ising universality class, *Phys. Rev. B* **82**, 174433 (2010).
- [67] M. V. Kompaniets and E. Panzer, Minimally subtracted six-loop renormalization of $O(n)$ -symmetric φ^4 theory and critical exponents, *Phys. Rev. D* **96**, 036016 (2017).
- [68] M. Campostrini, A. Pelissetto, P. Rossi, and E. Vicari, 25th-order high-temperature expansion results for three-

- dimensional Ising-like systems on the simple-cubic lattice Phys. Rev. E **65**, 066127 (2002).
- [69] R. Guida and J. Zinn-Justin, Critical exponents of the N-vector model, J. Phys. A **31**, 8103 (1998).
- [70] U. Wolff, Collective Monte Carlo Updating for Spin Systems, Phys. Rev. Lett. **62**, 361 (1989).
- [71] M. Hasenbusch and K. Pinn, A_+/A_- , α , ν , and $f_s \xi^3$ from 3D Ising energy and specific heat, J. Phys. A **31**, 6157 (1998).
- [72] M. Hasenbusch, K. Pinn, and S. Vinti, Critical exponents of the 3D Ising universality class from finite size scaling with standard and improved actions, Phys. Rev. B **59**, 11471 (1999).
- [73] A. Pelissetto, D. Rossini, and E. Vicari, Dynamic finite-size scaling after a quench at quantum transitions, Phys. Rev. E **97**, 052148 (2018).
- [74] H. Dorn, Renormalization of Path Ordered Phase Factors and Related Hadron Operators in Gauge Field Theories, Fortschr. Phys. **34**, 11 (1986).
- [75] S. Weinberg, *The Quantum Theory of Fields. Volume I. Foundations*, (Cambridge University Press, 2005).
- [76] S. Weinberg, *The Quantum Theory of Fields. Volume II. Modern Applications*, (Cambridge University Press, 2005).
- [77] M. Creutz, *Quarks, Gluons and Lattices*, (Cambridge University Press, 1983).
- [78] I. Montvay and G. Munster, *Quantum Fields on a Lattice*, (Cambridge University Press, 1994).
- [79] M. Lüscher, Properties and uses of the Wilson flow in lattice QCD, JHEP 08 (2010) 071.
- [80] M. Lüscher and P. Weisz, Perturbative analysis of the gradient flow in non-abelian gauge theories, JHEP 02 (2011) 051.
- [81] R. V. Harlander and T. Neumann, The perturbative QCD gradient flow to three loops, JHEP 06, 161 (2016).
- [82] F. Tarantelli and E. Vicari, Out-of-equilibrium dynamics arising from slow round-trip variations of Hamiltonian parameters across quantum and classical critical points, Phys. Rev. B **105**, 235124 (2022).
- [83] D. Rossini and E. Vicari, Interplay between short-range and critical long-range fluctuations in the out-of-equilibrium behavior of the particle density at quantum transitions, Phys. Rev. B **110**, 035126 (2024).
- [84] M. Campostrini, A. Pelissetto, P. Rossi, and E. Vicari, The two-point correlation function of three-dimensional O(N) models: critical limit and anisotropy, Phys. Rev. E **57**, 184 (1998).
- [85] D. Simmons-Duffin, The lightcone bootstrap and the spectrum of the 3D Ising CFT, JHEP 03 (2017) 086.